

Article

Multibeam Bathymetry and Distribution of Clay Minerals on Surface Sediments of a Small Bay in Terra Nova Bay, Antarctica

Jaewoo Jung ¹, Youngtak Ko ², Joochan Lee ³, Kiho Yang ⁴, Young Kyu Park ⁵, Sunghan Kim ⁶, Heungsoo Moon ⁶, Hyoung Jun Kim ³ and Kyu-Cheul Yoo ^{6,*}

- ¹ Global Ocean Research Center, Korea Institute of Ocean Science & Technology, Busan 49111, Korea; jaewoo@kiost.ac.kr
² Deep-Sea Mineral Resources Research Center, Korea Institute of Ocean Science & Technology, Busan 49111, Korea; ytko@kiost.ac.kr
³ Department of Future Technology Convergence, Korea Polar Research Institute, Incheon 21990, Korea; joochan@kopri.re.kr (J.L.); jun7100@kopri.re.kr (H.J.K.)
⁴ Department of Oceanography, Pusan National University, Busan 46241, Korea; kyang@pusan.ac.kr
⁵ Department of Earth System Sciences, Yonsei University, Seoul 03722, Korea; pyk125@yonsei.ac.kr
⁶ Division of Glacial Environment Research, Korea Polar Research Institute, Incheon 21990, Korea; delongksh@kopri.re.kr (S.K.); jepy@kopri.re.kr (H.M.)
* Correspondence: kcyoo@kopri.re.kr; Tel.: +82-10-3270-2998

Abstract: The second Antarctic station of South Korea was constructed at Terra Nova Bay, East Antarctica, but local seafloor morphology and clay mineralogical characteristics are still not fully understood. Its small bay is connected to a modern Campbell Glacier, cliffs, and raised beaches along the coastline. Fourteen sampling sites to collect surface sediments were chosen in the small bay for grain size and clay mineral analyses to study the sediment source and sediment-transport process with multibeam bathymetry and sub-bottom profiles. Under the dominant erosional features (streamlined feature and meltwater channel), icebergs are the major geological agent for transport and deposition of coarse-sized sediments along the edge of glaciers in summer, and thus the study area can reveal the trajectory of transport by icebergs. Glacier meltwater is an important agent to deposit the clay-sized detritus and it results from the dominance of the illite content occurring along the edge of Campbell Glacier Tongue. The high smectite content compared to Antarctic sediments may be a result of the source of the surrounding volcanic rocks around within the Melbourne Volcanic Province.

Keywords: Antarctica; Ross Sea; Terra Nova Bay; multibeam bathymetry; surface sediments; clay mineralogy



Citation: Jung, J.; Ko, Y.; Lee, J.; Yang, K.; Park, Y.K.; Kim, S.; Moon, H.; Kim, H.J.; Yoo, K.-C. Multibeam Bathymetry and Distribution of Clay Minerals on Surface Sediments of a Small Bay in Terra Nova Bay, Antarctica. *Minerals* **2021**, *11*, 72. <https://doi.org/10.3390/min11010072>

Received: 2 December 2020

Accepted: 11 January 2021

Published: 13 January 2021

Publisher's Note: MDPI stays neutral with regard to jurisdictional claims in published maps and institutional affiliations.



Copyright: © 2021 by the authors. Licensee MDPI, Basel, Switzerland. This article is an open access article distributed under the terms and conditions of the Creative Commons Attribution (CC BY) license (<https://creativecommons.org/licenses/by/4.0/>).

1. Introduction

The Ross Sea is adjacent to the Southern Ocean and is bounded by the Antarctic continent to the South. The Ross ice shelf, the largest ice shelf in Antarctica, is developed and distributed widely along the continental shelf [1]. The grounding line advanced near the continental shelf edge at the end of the Last Glacial Maximum (LGM, ca. 20 ka) and now is located within the Ross Sea [2,3]. The advance and retreat of the ice sheet caused by global climate change has had a significant impact on the depositional condition of the continental shelf [4]. Particularly, the Ross Sea is an important area for such study as the largest ice sheet that discharges into the embayment [5]. Terra Nova Bay, Ross Sea, is a bay which is often ice free, lying from Cape Washington in the north to the Drygalski Ice Tongue in the south [6]. Terra Nova Bay splits Victoria Land into southern and northern regions: (1) southern Victoria Land, where outlet glaciers and ice streams cross the Transantarctic Mountains and drain the East Antarctic Ice Sheet (EAIS) to the Ross Sea and (2) northern Victoria Land, where a dendritic pattern of glacial valleys has no direct connection to the EAIS, but is supplied by extensive ice fields [7,8]. Glaciomarine environments in high latitude regions are geologically important in that they contain the sedimentary history trapped

by their basin morphology that might preserve detailed paleoclimate history of Antarctic regions [9]. Acoustic surveys have been performed to understand glacier-influenced continental shelves in Ross Sea, Antarctica [10]. Multibeam bathymetric surveys to map the seafloor morphology of Antarctic regions have been used widely to identify glacial erosion of the seabed and other megascale glacial lineations related to ice sheet movement [11–13]. In order to determine the glaciomarine depositional environments, acoustic seafloor data have been collected from Ross Sea since 1990 [14–16]. The behavior of marine-based ice sheets across continental shelves was mostly reported and interpreted using regional seafloor bathymetric data [10,17] and satellite-based observations [18]. However, the local seafloor morphology and mineralogical characteristics of Terra Nova Bay have never been reported, so we provide general geological information including new multibeam bathymetry, sub-bottom profiles (SBP), grain size, clay mineralogy, and full width at half maximum 10 Å peak of illite/muscovite (FWHM-10 Å) for future study based on the Antarctic station. In the Antarctic region, the mineralogical characteristics of clay minerals in continental shelf sediments have been used successfully to describe the provenance of clay minerals and stratigraphic correlations in catchment areas draining into the Weddell Sea, Bellingshausen Sea, and Amundsen Sea, Antarctica [19–21]. The clay minerals that are common to Antarctic marine sediments include smectite, illite, chlorite, kaolinite, and illite-smectite(I-S) mixed layered clay [22,23]. These clay minerals are generally detrital and their distribution is affected by the the bedrock composition of source area [24]. The present study demonstrates a comprehensive understanding through geomorphological data, sedimentary sequences, grain size distributions, and clay mineralogy of surface sediments, where the second Antarctic station of South Korea was constructed. Then, this information contributes to interpreting those sediment-transport processes that influence sedimentation in Antarctic glaciomarine environments for future study.

2. Study Area

The study area in Terra Nova Bay of the Ross Sea was located offshore within 20 km from Jang Bogo Station (JBS) and Mario Zucchelli Station (MZS) (Figure 1). Seasonal sea ice, approximately 2 to 2.5 m thick, covers the sea surface for nine to ten months of the year. Terra Nova Bay has a winter coastal polynya. The inner bay of the study area is Gerlache Inlet between JBS and MZS. Tethys bay near MZS is a small cove (1.6 km wide and 3.0 km long), is very deep (a maximum depth of 280 m), and is surrounded by steep rocks and glaciers. The coastline from MZS to JBS is characterized by rocky cliffs with large boulders forming raised beaches. The raised beaches are present on the coast south of JBS and are composed dominantly of angular and sub-angular boulders formed by wave activity [25]. Campbell Glacier is located east of the JBS and is approximately 100 km long and approximately 4000 km² in the basin area. The Campbell Glacier Tongue (CGT), approximately 75.5 km² in surface area, is composed of one main stream (approximately 13.5 km long measured from the grounding line and 4.5 km wide) and another branched stream [26]. Air temperature varies from −30 to 5 °C annually, according to the measurement by an Automatic Weather Station installed at JBS.

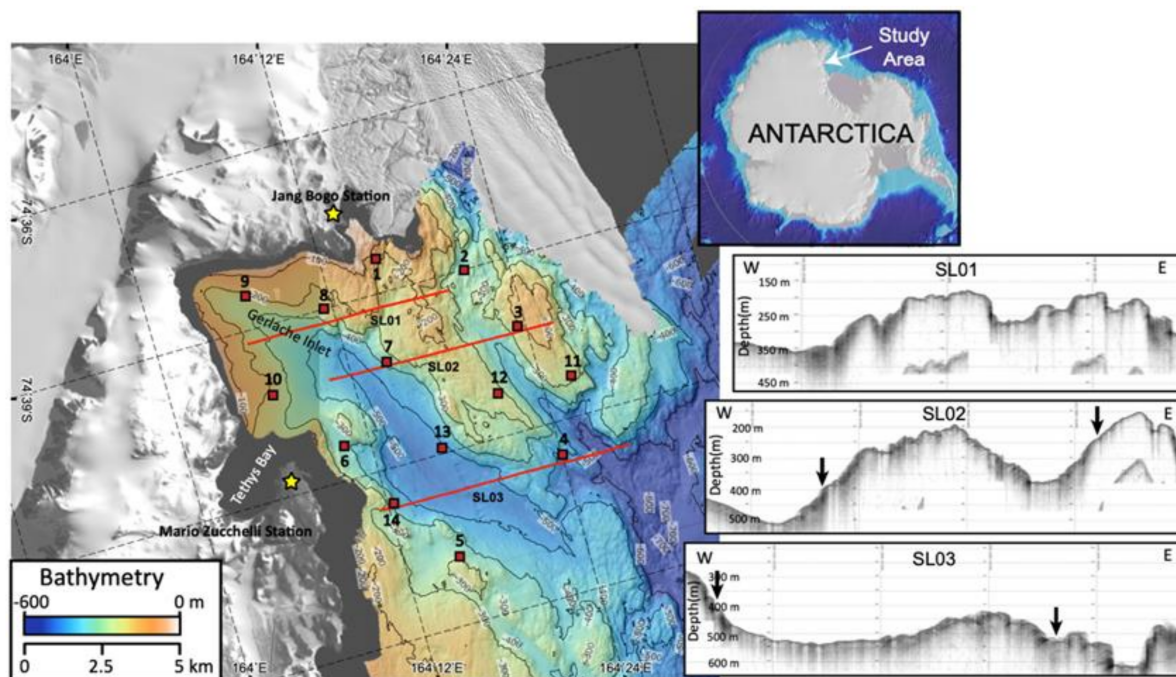


Figure 1. Sampling location, multibeam bathymetry data, and sub-bottom profiles of Terra Nova Bay, Antarctica. The arrows on the sub-bottom profiles indicate coring stations.

3. Materials and Methods

3.1. Sampling Locations

To understand the surface sediment characteristics in the glacial embayment adjacent to JBS in Terra Nova Bay, 14 sampling sites were chosen. However, 11 surface sediments were obtained using a box corer during the Ross Sea geological expedition in 2019 by the Korea Polar Research Institute (KOPRI) (Figure 1). Soft sediment at the three sampling sites (JBG05, JBG09 and JBG11) was not acquired, and some gravel or failed samples from the box corer indicated that the sites are likely till or rocky bottoms. Water depths at these sites vary between 150 and 523 m (Table 1). The sampling locations are given in Table 1.

Table 1. Sampling location and type of samples collected from Terra Nova Bay, Ross Sea, Antarctica.

Sampling Site	Latitude (S)	Longitude (E)	Water Depth (m)	Type of Sample
JBG01	74°38.40	164°15.60	150	Sediment
JBG02	74°39.00	164°21.00	390	Sediment
JBG03	74°40.20	164°23.40	225	Sediment
JBG04	74°42.60	164°24.00	523	Sediment
JBG05	74°43.80	164°15.60	328	Rocky bottom
JBG06	74°41.40	164°10.20	386	Sediment
JBG07	74°40.20	164°14.40	390	Sediment
JBG08	74°39.00	164°11.40	255	Sediment
JBG09	74°38.40	164°06.60	230	Rocky bottom
JBG10	74°40.20	164°06.60	235	Sediment
JBG11	74°41.27	164°25.93	280	Rocky bottom
JBG12	74°41.25	164°20.99	270	Sediment
JBG13	74°41.90	164°16.44	515	Sediment
JBG14	74°42.60	164°12.37	388	Sediment

3.2. Multibeam Bathymetry and Sub-Bottom Profiles

Multibeam swath bathymetry data were collected during a geophysical research expedition near JBS aboard the RV/IB Araon. Multibeam soundings were collected in a swath perpendicular to the ship track using a hull-mounted Kongsberg EM122 (Kongsberg Maritime, Kongsberg, Norway), with a swath of 432 beams, operating at a frequency of 12 KHz. Acquired bathymetry data were processed onboard using CARIS (HIPS&SIPS 9.0, Teledyne CARIS, Fredericton, NB, Canada), specialized bathymetry-processing software, and the results were plotted using Generic Mapping Tools (GMT 6.1.1, School of Ocean and Earth Science and Technology of University of Hawaii at Manoa, HI, USA) software. To understand ice flow activity, we compared the submarine landforms to the seafloor lithology based on sub-bottom profiling results. Shallow sub-bottom profiling data were collected in the sampling area using an SBP120 Sub-bottom profiler with an optional extension to the highly acclaimed EM122 multibeam echo sounder. The data were logged in the TOPAS raw format and can be saved in SEG-Y format for postprocessing with a standard seismic package. The data were used to identify seafloor lithology and the thickness of surface sedimentary units (unconsolidated sediments up to 100 m below the seafloor).

3.3. Analysis of Grain Size and Clay Mineralogy

Grain size analysis of surface sediments was performed to determine the size fractions of gravel (>2 mm), sand (62.5 μm to 2 mm), silt (2 μm to 62.5 μm), and clay (<2 μm) [27]. The contents of coarse particles larger than 4ϕ (>62.5 μm) were determined by wet sieving, and particles smaller than 62.5 μm were measured using Micromeritics SediGraph III 5120 (Micromeritics Instrument Corporation, Norcross, GA, USA). X-ray diffraction (XRD) analysis was performed using a Rigaku HR-XRD SmartLab (Rigaku, Tokyo, Japan) with Cu-K α radiation (20 kV and 10 mA). The XRD profiles over a range of 2θ angles from 2° to 70° were measured at step sizes of 0.02° and a scan speed of $1.5^\circ/\text{min}$. Size-fractionated samples (<1 μm) were dispersed in deionized water (0.5 mg/mL) and put in an ultrasonicator bath for 20 s to prevent particle flocculation. The oriented (air-dried) samples were placed onto glass slides for XRD analysis [20]. Then, air-dried samples were treated with ethylene-glycol under a vacuum desiccator for 48 h [28,29]. Quantitative estimations of clay minerals were measured after the glycolation treatment. The relative percentage of each clay mineral was calculated using weighting factors [29,30]. Search-Match software (version 2.0.3.1, Oxford Cryosystems, Oxford, UK) was used to identify the clay mineralogy [31]. FWHM-10 \AA [32] and the relative percentage of smectite, chlorite, illite, and kaolinite were measured and calculated by using *OriginPro 2020b* [20,28].

4. Results

4.1. Geomorphology

We described the seafloor landforms identified in the sampling area [33]. Gerlache Inlet (a maximum depth of 350 m) located between JBS and MZS is surrounded by steep bedrocks and glaciers in the western side. Tethys Bay, adjacent to MZS, is very deep (about 280 m water depth in the central part). The sampling area is characterized by a rugged seafloor with meltwater channels west of CGT and a large (7.3 km²), deep (520 m water depth) flat-bottomed basin east of MZS (Figure 2). Elongated streamlined features are found west of CGT. In the sub-bottom profiles, the sampling area shows a strong surface with no internal reflectors (Figure 1). The meltwater channels have a V-shaped cross-sectional profile cutting through bedrock and flowing between the streamlined features. The reticular channels between streamlined features mainly terminate beneath CGT, and the arboriform channels in the offshore of the JBS terminate in the deep basin.

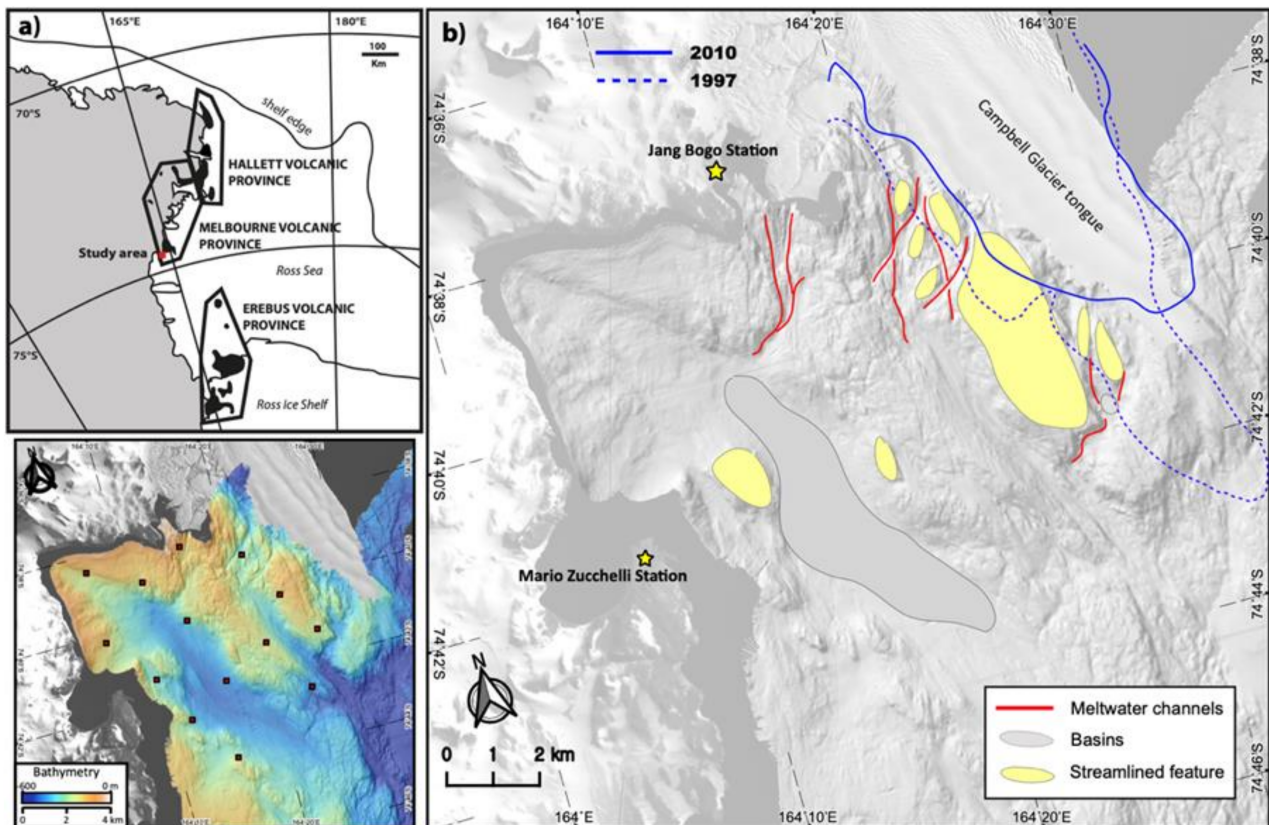


Figure 2. Multibeam swath bathymetry and geomorphology of the study area. (a) The study area is included in the Melbourne Volcanic Province. (b) The solid line is the boundary of CGT [34] and the dotted line [35].

4.2. Granulometric Composition

Table 2 shows the results obtained by grain size analysis of the surface sediment samples. The sediments of sampling sites are largely coarse-grained. Sand contents generally exceed 87.5% except at JBG03 and JBG13, while mud (silt + clay) contents do not exceed 9.3% except at JBG13 (27.0%). JBG03 has large amounts of gravel (35.4%), while the gravel contents of other sites are relatively low (<6.2%). The sediment is generally moderately sorted to very poorly sorted (0.7 to 3.2 ϕ). The mean grain size is generally medium sand (1.7 ϕ) to very fine sand (3.2 ϕ) except for very coarse sand (0.5 ϕ) at JBG03 and coarse silt at JBG13 (5.1 ϕ). The components more coarse than medium sand, a combination of gravel, coarse sand, and medium sand contents, were examined to distinguish coarser fractions from finer fractions of grain size distribution in the surface sediments. The coarser components of JBG02, JBG03, and JBG04 exceed approximately 49.1%, while other sites show low contents below 32.5%.

Table 2. Grain size distribution of surface sediments collected from Terra Nova Bay, Ross Sea, Antarctica.

Sampling Site	Gravel (%)	Sand (%)	Silt (%)	Clay (%)	Gravel + Coarse/Medium Sand (%)	Mean Size (ϕ)	Sorting (ϕ)
JBG01	0.2	89.9	5.2	4.7	10.1	3.0	1.4
JBG02	6.2	88.1	2.8	2.9	49.1	1.9	1.8
JBG03	35.4	61.0	1.4	2.5	68.3	0.5	2.4
JBG04	0.1	99.5	0.1	0.2	73.6	1.7	0.7
JBG06	3.2	95.0	0.6	1.2	32.5	2.4	1.1
JBG07	0.6	90.1	3.7	5.6	13.3	3.2	1.7
JBG08	0.0	87.5	7.2	5.3	9.6	3.2	1.5
JBG10	0.0	91.9	1.4	6.7	5.3	3.2	1.6
JBG12	0.1	97.2	1.0	1.8	24.5	2.5	0.9
JBG13	0.0	73.0	10.0	17.0	9.3	5.1	3.2
JBG14	0.0	95.9	1.3	2.7	15.8	2.8	0.8

4.3. Semi-Quantification of Clay Minerals and Full Width at Half Maximum of Illite

Oriented and ethylene-glycolated samples were used to determine the clay mineralogy in sediments. In general, the mineralogical assemblages evidenced in surface sediment samples collected at Terra Nova Bay (Figure 1) were expandable clay minerals (smectite (S) and/or mixed layers illite-smectite R0), chlorite (Ch), illite (I), kaolinite (K), plagioclase (Pl), and clay-sized quartz (Q). Unfortunately, JBG04 and JBG10 have no results because there were no samples to conduct clay mineral analysis after grain size analysis. A slight peak was observed between 9–10 2-theta degrees, indicating an I-S mixed layer. There were no significant mineralogical variations with a distance from the coastline. The average clay mineral composition was dominated by illite (53.7–74.0%, avg. = 64.9%) and chlorite (10.0–16.8%, avg. = 12.8%) with less abundant clay minerals of smectite (6.5–20.1%, avg. = 12.4%) and kaolinite (7.0–13.8%, avg. = 10.0%, Table 3). The relative peak intensity of the minerals showed little difference in intensities through Terra Nova Bay, but the intensities of quartz peaks increased in JBG08 compared to other sites (Figure 3). In addition, smectite peaks (~17 Å) were very weak at JBG 08, corresponding to the lowest concentration of smectite (6.46%). The values of FWHM-10 Å in $^{\circ}\Delta 2\theta$ show a narrow variation with sampling location ranging from 0.40–0.54 and an average value of 0.47.

Table 3. Relative abundance of clay minerals and full width at half maximum 10 Å peak of illite/muscovite (FWHM-10 Å) of surface sediments collected from Terra Nova Bay, Antarctica.

Sampling Site	Smectite (%)	Illite (%)	Kaolinite (%)	Chlorite (%)	FWHM ($^{\circ}\Delta 2\theta$)
JBG01	8.6	74.0	7.5	10.0	0.49
JBG02	12.0	67.7	7.8	12.6	0.52
JBG03	11.2	71.3	7.0	10.6	0.49
JBG06	12.7	58.4	13.0	15.9	0.43
JBG07	13.8	65.3	9.3	11.6	0.48
JBG08	6.5	70.3	10.9	12.4	0.41
JBG09	12.9	62.3	11.7	13.2	0.47
JBG12	10.6	69.2	9.1	11.1	0.42
JBG13	15.7	53.7	13.8	16.8	0.40
JBG14	20.1	56.5	9.6	13.8	0.54
Avg.	12.3	64.6	10.0	12.8	0.47

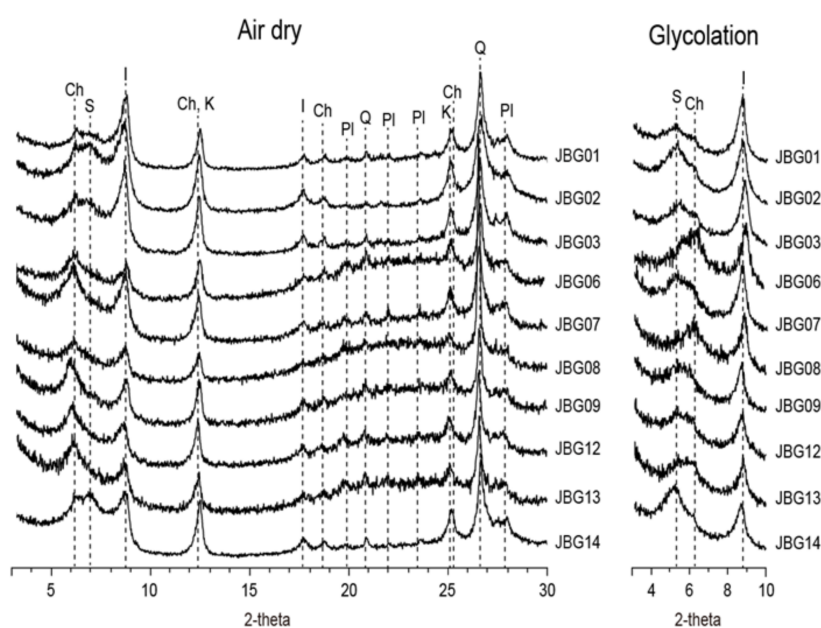


Figure 3. The XRD profiles of air-dried and glycolate-treated clay (<1 μm) in surface sediments from Terra Nova Bay (S: smectite, Ch: chlorite, I: illite, K: kaolinite, Pl: plagioclase, Q: quartz).

5. Discussion

The investigation of clay mineralogy in surface sediments recorded from the proximal zone of the coastline provides evidence of source areas and transport paths. In a polar setting, physical weathering prevails and chemical weathering is negligible. Detrital clay mineral assemblages in the surface sediments reflect the average rock composition in the surrounding outcrops [23]. In particular, illite and chlorite are typical clay minerals indicating the physical weathering in the soil environments [24]. The dominance of illite in the sampling area (Figure 4) likely reflects the supply of detritus from outcrops of the local sources, because clay mineral assemblages in the surface sediments are formed by the weathering of the outcrops [36]. The narrow variation of FWHM values ($^{\circ}\Delta 2\theta = 0.40\text{--}0.54$, avg. = 0.47) indicates the good crystallinity of illite which is less-altered illite close to the surface. The chemical index of illite (5/10 Å peak area ratio) less influenced by sediment dynamic differentiation was ~ 0.2 (calculated from Figure 3), indicating that Fe–Mg-rich illite resulted from the physical weathering of bedrocks [23,37], suggesting that the illite originated in dry and cold environments. Furthermore, the clay-sized fraction of quartz and plasioclase suggests little chemical weathering of glacially-derived source materials [38]. It may have resulted from the glaciomarine environment of the study area, characterized by a limited moisture supply and short summer season, which do not enhance chemical weathering.

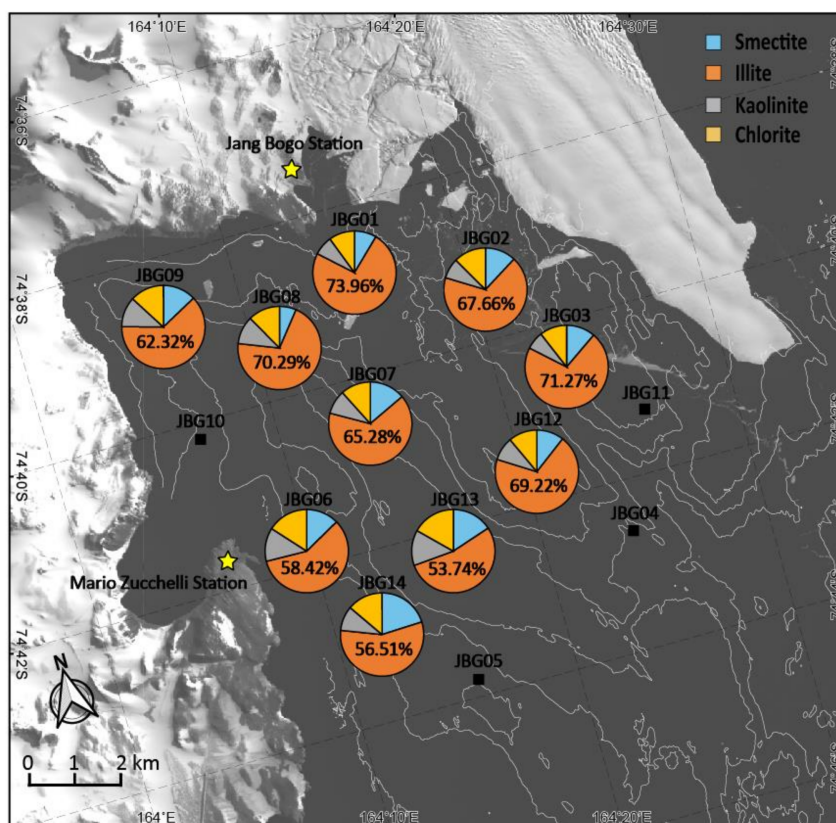


Figure 4. Average clay mineral composition of surface sediments collected from Terra Nova Bay, Antarctica.

On the other hand, expandable minerals (smectite and/or mixed layers illite-smectite R0) were derived from hydrothermal alteration of volcanic ash supplied from the surrounding areas or weathering and erosion of exposed volcanic rocks [39]. The content of expandable minerals is relatively high in the quaternary sediments, indicating that sediments originated from basic volcanic rocks in the Ross Sea area [40]. This is consistent with the previous study, i.e., that the smectite distributed in the Ross Sea was supplied by the

McMurdo Volcanic Group on the coast of Victoria Land [41]. The content of smectite in the study area (Table 3) is largely high compared to general Antarctic marine sediments with a relatively low content of smectite. The Melbourne Volcanic Province, a member of the McMurdo Volcanic Group, is divided into four subprovinces: Malta Plateau, the Pleiades, Mount Overlord, and Mount Melbourne. The study area is situated about 30 km away from Mount Melbourne that is in the center of Mount Melbourne subprovince adjacent to the CGT, and so smectite in the sampling sites may have originated from the outcrops (Figure 2a) [42,43]. Kaolinite is very resistant, and reworked kaolinite from older sediments may be found in polar environments [22,43]. Kaolinite might be derived from the paleosol and sedimentary rocks containing kaolinite near the Ross Sea, but it is still not fully understood. For this reason, it is necessary to determine the provenance of clay minerals more clearly through the analysis of rare earth elements (REE), sand fraction by optical microscopy, and Scanning Electron Microscopy of the sediments [44,45].

Surface sediments provide a useful material to reveal how modern environmental conditions are reflected, especially in transportation and depositional processes of clastic materials farther offshore from the surrounding sources. The analysis of the grain size of surface sediments showed that the finer components (silt and clay) of all sampling sites are very low. This indicates that the silt- and clay-sized components on the surface sediments of all sites are involved in an insignificant sedimentary process. The study area is free from sea ice only from the beginning of January to the end of February. In fact, there is no river on the local coast and little turbid onshore meltwater streams entering the ocean since the study area is located at a high latitude in a polar setting. However, the relative illite abundance is higher on the surface sediments close to CGT, suggesting that illite is derived from the meltwater input of CGT in summer. Strong winds are frequent from the hinterland in winter. They result in the rugged surface (e.g., crevasses) of glaciers due to physical weathering in winter, and thus the clay fraction may deposit along the edge of CGT through the direct glacier meltwater in summer. The fine-sized detrital components can be transported farther seaward by ocean currents. It turns out that surface sediments in the deep basin (e.g., Drygalski Basin) of Terra Nova Bay predominantly consist of mud. Some fine-sized components are likely to be transported into the study area alongshore by ocean currents. There is prevailing north-eastward alongshore transport between the surface and deep layers from current measurements in Terra Nova Bay [46].

Elongated streamlined features or elongated hills are found near CGT (Figure 2) with no internal hummocky reflection in the sub-bottom profiles (Figure 1). Linear and sinuous meltwater channels are more frequent near CGT. Streamlined features and meltwater channels are erosional seafloor features, which likely indicate till and/or bedrock. Multiple glaciation events are likely to allow actively flowing ice to carve into the bedrock [47]. It is reported that some of the proximal areas are modern erosional features when ice recently advanced [33]; some at the proximal bay in front of JBS and the surrounding CGT likely formed during a recent glacial event, the Little Ice Age. On the other hand, a deep basin shows a very thin drape overlying a strong reflection on line SL03 (Figure 1). JBG13 has more abundant mud contents than other sites and is a representative deposition site of fine-sized components among all sampling sites (Table 2).

The coarse components (gravel + sand) are largely supplied from the source rocks (Late Precambrian metamorphic rocks and Late Cenozoic Volcanics) fringing the coast of the sampling area. The dominance of coarse components occurs at all sites except at JBG13. It can be considered that one of the dominant transport media for coarse-sized material into the study area is sediment gravity flow, especially turbid currents [48]. However, the study area has no hydraulic potential to yield density flow such as the continental slope and no sedimentary sequence of density flow in the sub-bottom profiles. Another possible transport medium is the ice-rafted materials supplied to the ocean by drifting icebergs from the glaciers of the surrounding sources. The components more coarse than medium sand become one of the criteria of ice-rafted transport because sometimes eolian transport from the surrounding outcrops can be composed of large-sized materials (>4 μm

fine sand) [49]. The main source of ice-rafted detritus is from the Campbell Glacier that largely releases small-scale icebergs to the study area with increased temperature ($>0\text{ }^{\circ}\text{C}$) in summer. The terminus of CGT retreated about 4.4 km between 1984 and 2016 due to local warming [50]. The dominance of the components more coarse than medium sand along the edge of CGT (Figure 5) may result from the deposition of ice-rafted detritus in summer. The coarse components of the JBG06 and JBG14 sites in front of MZS are likely due to the surrounding glaciers, especially in Tethys Bay. It was reported that the seafloor is primarily granitic rock composed of coarse sand or gravel [51].

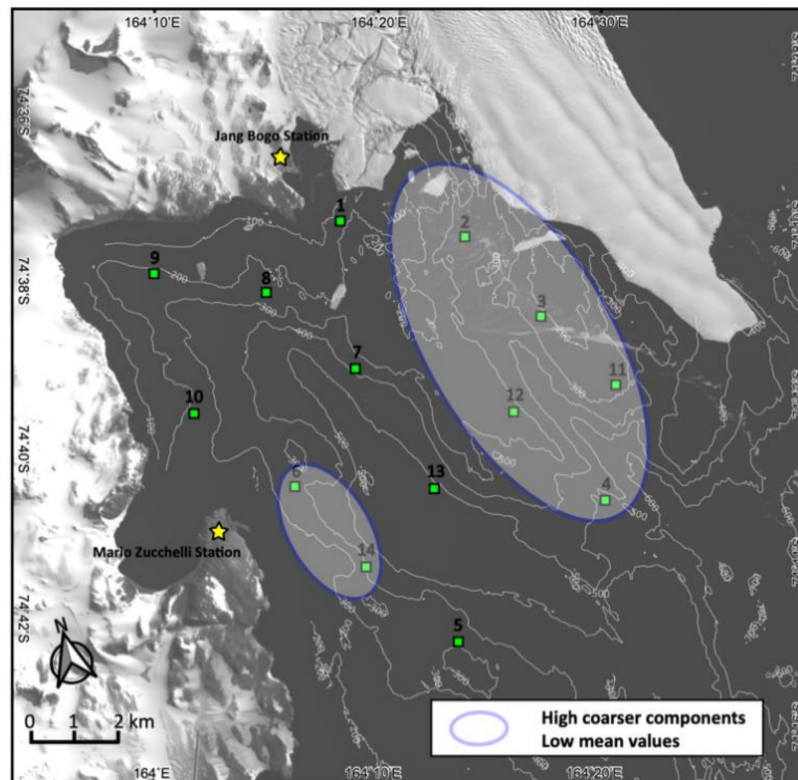


Figure 5. The relative mean size and coarse-sized component of surface sediments.

6. Conclusions

Systematic analysis of the grain size and clay minerals in glaciomarine surface sediments delivered to a small bay of Terra Nova Bay was performed with geophysical characteristics from bathymetry and sub-bottom profiles. Our findings suggest the sediment-transport processes of glaciogenic detritus under the influence of recent regional warming. The following conclusions are presented:

1. The relative abundance of clay minerals in the surface sediments of the study area is largely dominated by illite, reflecting the supply of physical weathering products from the surrounding outcrops. The expandable mineral (smectite and/or mixed layers illite-smectite R0) content is largely high compared to general Antarctic marine sediments, indicative of delivery of products of weathering and erosion of exposed volcanic rocks from the Melbourne Volcanic Province close to the sampling sites.
2. Erosional features (streamlined features and meltwater channels) are found near CGT with many coarse-sized components compared with medium sand on till and/or bedrock except in a deep basin representing a deposition area of fine-sized components in the study area.
3. Clastic materials are mainly transported offshore into the sampling site through two agents: icebergs and glacier meltwater. Icebergs detached from the surrounding glaciers mainly deposit the gravel and medium/coarse sand components ($>49.1\%$)

on the rugged bedrocks along the edge of CGT and offshore near the coastline of Tethys Bay. When the study area is free from sea ice for about two months in summer, some wind-blown materials (fine sand and silt components) are transported into the sampling sites. Glacier melting occurs in summer, and the clay-sized component of physical weathering products from the surrounding land is deposited along the edge of CGT.

Author Contributions: J.J. designed the study concept and contributed to manuscript preparation. K.Y. and Y.K.P. contributed to XRD data production and S.K. to grain size analysis. H.M. contributed to fieldwork and sample collection. J.L., H.J.K. and Y.K. produced multibeam and SBP data. K.-C.Y. revised the manuscript. All authors have read and agreed to the published version of the manuscript.

Funding: This work was funded by a Korea Polar Research Institute (KOPRI) project (PE21090) awarded to K.-C.Y.

Institutional Review Board Statement: Not applicable.

Informed Consent Statement: Not applicable.

Data Availability Statement: The data that support the findings of this study are available from the corresponding author, upon reasonable request.

Conflicts of Interest: The authors declare no conflict of interest.

References

- Rignot, E.; Jacobs, S.; Mouginot, J.; Scheuchl, B. Ice-shelf melting around Antarctica. *Science* **2013**, *341*, 266–270. [[CrossRef](#)] [[PubMed](#)]
- Howat, I.M.; Domack, E.W. Reconstructions of western Ross Sea palaeo-ice-stream grounding zones from high-resolution acoustic stratigraphy. *Boreas* **2003**, *32*, 56–75. [[CrossRef](#)]
- Anderson, J.B.; Conway, H.; Bart, P.J.; Witus, A.E.; Greenwood, S.L.; McKay, R.M.; Hall, B.L.; Ackert, R.P.; Licht, K.; Jakobsson, M. Ross Sea paleo-ice sheet drainage and deglacial history during and since the LGM. *Quat. Sci. Rev.* **2014**, *100*, 31–54. [[CrossRef](#)]
- Domack, E.W.; Jacobson, E.A.; Shipp, S.; Anderson, J.B. Late Pleistocene–Holocene retreat of the West Antarctic Ice-Sheet system in the Ross Sea: Part 2—Sedimentologic and stratigraphic signature. *Geol. Soc. Am. Bull.* **1999**, *111*, 1517–1536. [[CrossRef](#)]
- Setti, M.; Marinoni, L.; Lopez-Galindo, A. Mineralogical and geochemical characteristics (major, minor, trace elements and REE) of detrital and authigenic clay minerals in a Cenozoic sequence from Ross Sea, Antarctica. *Clay Miner.* **2004**, *39*, 405–421. [[CrossRef](#)]
- Di Nicola, L.; Strasky, S.; Schlüchter, C.; Salvatore, M.C.; Akçar, N.; Kubik, P.W.; Christl, M.; Kasper, H.U.; Wieler, R.; Baroni, C. Multiple cosmogenic nuclides document complex Pleistocene exposure history of glacial drifts in Terra Nova Bay (northern Victoria Land, Antarctica). *Quat. Res.* **2009**, *71*, 83–92. [[CrossRef](#)]
- Orombelli, G. Terra Nova Bay: A geographic overview. *Mem. Della Soc. Geol. Ital.* **1987**, *33*, 69–75.
- Baroni, C.; Noti, V.; Ciccacci, S.; Righini, G.; Salvatore, M.C. Fluvial origin of the valley system in northern Victoria Land (Antarctica) from quantitative geomorphic analysis. *Geol. Soc. Am. Bull.* **2005**, *117*, 212–228. [[CrossRef](#)]
- Mosola, A.B.; Anderson, J.B. Expansion and rapid retreat of the West Antarctic Ice Sheet in eastern Ross Sea: Possible consequence of over-extended ice streams? *Quat. Sci. Rev.* **2006**, *25*, 2177–2196. [[CrossRef](#)]
- Halberstadt, A.R.W.; Simkins, L.M.; Greenwood, S.L.; Anderson, J.B. Past ice-sheet behaviour: Retreat scenarios and changing controls in the Ross Sea, Antarctica. *Cryosphere* **2016**, *10*, 1003–1020. [[CrossRef](#)]
- Lee, J.I.; McKay, R.M.; Gолledge, N.R.; Yoon, H.I.; Yoo, K.-C.; Kim, H.J.; Hong, J.K. Widespread persistence of expanded East Antarctic glaciers in the southwest Ross Sea during the last deglaciation. *Geology* **2017**, *45*, 403–406. [[CrossRef](#)]
- Shipp, S.; Anderson, J.B. Drumlin field on the Ross Sea continental shelf, Antarctica. In *Glaciated Continental Margins*; Springer: Berlin/Heidelberg, Germany, 1997; pp. 52–53.
- Dowdeswell, J.; Ottesen, D.; Evans, J.; Cofaigh, C.; Anderson, J. Submarine glacial landforms and rates of ice-stream collapse. *Geology* **2008**, *36*, 819–822. [[CrossRef](#)]
- Cooper, A.K.; Barrett, P.J.; Hinz, K.; Traube, V.; Letichenkov, G.; Stagg, H.M. Cenozoic prograding sequences of the Antarctic continental margin: A record of glacio-eustatic and tectonic events. *Mar. Geol.* **1991**, *102*, 175–213.
- De Santis, L.; Prato, S.; Brancolini, G.; Lovo, M.; Torelli, L. The Eastern Ross Sea continental shelf during the Cenozoic: Implications for the West Antarctic ice sheet development. *Glob. Planet. Chang.* **1999**, *23*, 173–196. [[CrossRef](#)]
- Salvini, F.; Brancolini, G.; Busetto, M.; Storti, F.; Mazzarini, F.; Coren, F. Cenozoic geodynamics of the Ross Sea region, Antarctica: Crustal extension, intraplate strike-slip faulting, and tectonic inheritance. *J. Geophys. Res. Solid Earth* **1997**, *102*, 24669–24696. [[CrossRef](#)]
- Greenwood, S.L.; Gyllencreutz, R.; Jakobsson, M.; Anderson, J.B. Ice-flow switching and East/West Antarctic Ice Sheet roles in glaciation of the western Ross Sea. *Bulletin* **2012**, *124*, 1736–1749. [[CrossRef](#)]

18. Brunt, K.M.; Fricker, H.A.; Padman, L.; Scambos, T.A.; O'Neel, S. Mapping the grounding zone of the Ross Ice Shelf, Antarctica, using ICESat laser altimetry. *Ann. Glaciol.* **2010**, *51*, 71–79. [[CrossRef](#)]
19. Hillenbrand, C.-D.; Grobe, H.; Diekmann, B.; Kuhn, G.; Fütterer, D.K. Distribution of clay minerals and proxies for productivity in surface sediments of the Bellingshausen and Amundsen seas (West Antarctica)—Relation to modern environmental conditions. *Mar. Geol.* **2003**, *193*, 253–271. [[CrossRef](#)]
20. Jung, J.; Yoo, K.-C.; Lee, K.-H.; Park, Y.K.; Lee, J.I.; Kim, J. Clay mineralogical characteristics of sediments deposited during the late quaternary in the Larsen ice shelf B embayment, Antarctica. *Minerals* **2019**, *9*, 12. [[CrossRef](#)]
21. Park, Y.K.; Lee, J.I.; Jung, J.; Hillenbrand, C.-D.; Yoo, K.-C.; Kim, J. Elemental compositions of smectites reveal detailed sediment provenance changes during glacial and interglacial periods: The Southern Drake Passage and Bellingshausen Sea, Antarctica. *Minerals* **2019**, *9*, 322. [[CrossRef](#)]
22. Chamley, H. *Clay Sedimentology*; Springer: New York, NY, USA, 2013.
23. Petschick, R.; Kuhn, G.; Gingele, F. Clay mineral distribution in surface sediments of the South Atlantic: Sources, transport, and relation to oceanography. *Mar. Geol.* **1996**, *130*, 203–229. [[CrossRef](#)]
24. Ehrmann, W.U.; Melles, M.; Kuhn, G.; Grobe, H. Significance of clay mineral assemblages in the Antarctic Ocean. *Mar. Geol.* **1992**, *107*, 249–273. [[CrossRef](#)]
25. Hong, S.; Lee, M.K.; Seong, Y.B.; Owen, L.A.; Rhee, H.H.; Lee, J.I.; Yoo, K.-C. Holocene sea-level history and tectonic implications derived from luminescence dating of raised beaches in Terra Nova Bay, Antarctica. *Geosci. J.* **2020**, 1–16. [[CrossRef](#)]
26. Han, H.; Lee, H. Tide deflection of Campbell Glacier Tongue, Antarctica, analyzed by double-differential SAR interferometry and finite element method. *Remote Sens. Environ.* **2014**, *141*, 201–213. [[CrossRef](#)]
27. Jones, K.; McCave, I.; Patel, D. A computer-interfaced sedigraph for modal size analysis of fine-grained sediment. *Sedimentology* **1988**, *35*, 163–172. [[CrossRef](#)]
28. Jung, J.; Yoo, K.-C.; Rosenheim, B.E.; Conway, T.M.; Lee, J.I.; Yoon, H.I.; Hwang, C.Y.; Yang, K.; Subt, C.; Kim, J. Microbial Fe (III) reduction as a potential iron source from Holocene sediments beneath Larsen Ice Shelf. *Nat. Commun.* **2019**, *10*, 1–10.
29. Biscaye, P.E. Distinction between kaolinite and chlorite in recent sediments by X-ray diffraction. *Am. Mineral. J. Earth Planet. Mater.* **1964**, *49*, 1281–1289.
30. Biscaye, P.E. Mineralogy and sedimentation of recent deep-sea clay in the Atlantic Ocean and adjacent seas and oceans. *Geol. Soc. Am. Bull.* **1965**, *76*, 803–832. [[CrossRef](#)]
31. Yang, K.; Yoo, K.-C.; Jung, J. Quantitative analysis of asbestos-containing materials using various test methods. *Minerals* **2020**, *10*, 568. [[CrossRef](#)]
32. Guggenheim, S.; Bain, D.C.; Bergaya, F.; Brigatti, M.F.; Drits, V.A.; Eberl, D.D.; Formoso, M.L.; Galán, E.; Merriman, R.J.; Peacor, D.R. Report of the Association Internationale pour l'Etude des Argiles (AIPEA) Nomenclature Committee for 2001: Order, disorder and crystallinity in phyllosilicates and the use of the 'crystallinity index'. *Clay Miner.* **2002**, *37*, 389–393. [[CrossRef](#)]
33. Munoz, Y.P.; Wellner, J.S. Seafloor geomorphology of western Antarctic Peninsula bays: A signature of ice flow behaviour. *Cryosphere* **2018**, *12*, 205–225. [[CrossRef](#)]
34. Han, H.; Ji, Y.; Lee, H. Estimation of annual variation of ice extent and flow velocity of Campbell Glacier in East Antarctica using COSMO-SkyMed SAR images. *Korean J. Remote Sens.* **2013**, *29*, 45–55. [[CrossRef](#)]
35. Guglielmo, L.; Zagami, G.; Saggiomo, V.; Catalano, G.; Granata, A. Copepods in spring annual sea ice at Terra Nova Bay (Ross Sea, Antarctica). *Polar Biol.* **2007**, *30*, 747–758. [[CrossRef](#)]
36. Ehrmann, W.; Hillenbrand, C.-D.; Smith, J.A.; Graham, A.G.; Kuhn, G.; Larter, R.D. Provenance changes between recent and glacial-time sediments in the Amundsen Sea embayment, West Antarctica: Clay mineral assemblage evidence. *Antarct. Sci.* **2011**, *23*, 471–486. [[CrossRef](#)]
37. Wang, Q.; Yang, S. Clay mineralogy indicates the Holocene monsoon climate in the Changjiang (Yangtze River) Catchment, China. *Appl. Clay Sci.* **2013**, *74*, 28–36. [[CrossRef](#)]
38. Sinha, R.; Chatterjee, A. Mineralogy of lacustrine sediments in the Schirmacher range area, eastern Antarctica. *J. Geol. Soc. India* **2000**, *56*, 39–46.
39. Jeong, G.; Yoon, H. The origin of clay minerals in soils of King George Island, South Shetland Islands, West Antarctica, and its implications for the clay-mineral compositions of marine sediments. *J. Sediment. Res.* **2001**, *71*, 833–842. [[CrossRef](#)]
40. Jung, J.; Park, Y.; Lee, K.-H.; Hong, J.; Lee, J.; Yoo, K.-C.; Lee, M.; Kim, J. Clay Mineralogical Characteristics and Origin of Sediments Deposited during the Pleistocene in the Ross Sea, Antarctica. *J. Mineral. Soc. Korea* **2019**, *32*, 163–172. [[CrossRef](#)]
41. Salvi, C.; Busetti, M.; Marinoni, L.; Brambati, A. Late Quaternary glacial marine to marine sedimentation in the Pennell Trough (Ross Sea, Antarctica). *Palaeogeogr. Palaeoclimatol. Palaeoecol.* **2006**, *231*, 199–214. [[CrossRef](#)]
42. Ehrmann, W.; Setti, M.; Marinoni, L. Clay minerals in Cenozoic sediments off Cape Roberts (McMurdo Sound, Antarctica) reveal palaeoclimatic history. *Palaeogeogr. Palaeoclimatol. Palaeoecol.* **2005**, *229*, 187–211. [[CrossRef](#)]
43. Ehrmann, W. Lower Miocene and Quaternary clay mineral assemblages from CRP-1. *Terra Antart.* **1998**, *5*, 613–619.
44. Perri, F.; Critelli, S.; Cavalcante, F.; Mongelli, G.; Dominici, R.; Sonnino, M.; De Rosa, R. Provenance signatures for the Miocene volcaniclastic succession of the Tufiti di Tusa Formation, southern Apennines, Italy. *Geol. Mag.* **2012**, *149*, 423–442. [[CrossRef](#)]
45. Cavalcante, F.; Fiore, S.; Piccarreta, G.; Tateo, F. Geochemical and mineralogical approaches to assessing provenance and deposition of shales: A case study. *Clay Miner.* **2003**, *38*, 383–397. [[CrossRef](#)]

46. Buffoni, G.; Cappelletti, A.; Picco, P. An investigation of thermohaline circulation in Terra Nova Bay polynya. *Antarct. Sci.* **2002**, *14*, 83. [[CrossRef](#)]
47. Livingstone, S.J.; Cofaigh, C.Ó.; Stokes, C.R.; Hillenbrand, C.-D.; Vieli, A.; Jamieson, S.S. Glacial geomorphology of Marguerite Bay palaeo-ice stream, western Antarctic Peninsula. *J. Maps* **2013**, *9*, 558–572. [[CrossRef](#)]
48. Postma, G. Classification for sediment gravity-flow deposits based on flow conditions during sedimentation. *Geology* **1986**, *14*, 291–294. [[CrossRef](#)]
49. Chewings, J.M.; Atkins, C.B.; Dunbar, G.B.; Golledge, N.R. Aeolian sediment transport and deposition in a modern high-latitude glacial marine environment. *Sedimentology* **2014**, *61*, 1535–1557. [[CrossRef](#)]
50. Rhee, H.H.; Lee, M.K.; Seong, Y.B.; Hong, S.; Lee, J.I.; Yoo, K.-C.; Yu, B.Y. Timing of the local last glacial maximum in Terra Nova Bay, Antarctica defined by cosmogenic dating. *Quat. Sci. Rev.* **2019**, *221*, 105897. [[CrossRef](#)]
51. Pensieri, S.; Bozzano, R.; Schiano, M.E.; Pensieri, L.; Traverso, F.; Trucco, A.; Picco, P.; Bordone, A. Environmental acoustic noise observations in Tethys Bay (Terra Nova Bay, Ross Sea, Antarctica). In Proceedings of the 2014 Oceans-St. John's, St. John's, NL, Canada, 14–19 September 2014; pp. 1–6.